Mg-RICH SMECTITE "PRECURSOR" PHASE IN THE TAGUS BASIN, SPAIN

CRISTINA DE SANTIAGO BUEY,[1] MERCEDES SUÁREZ BARRIOS,[2] EMILIA GARCÍA ROMERO,[1] AND MERCEDES DOVAL MONTOYA[1]

[1]Departamento de Cristalografía y Mineralogía, Facultad de Ciencias Geológicas, UCM, Spain
[2]Departamento de Geología, Area de Cristalografía y Mineralogía, Facultad de Ciencias, Universidad de Salamanca, Spain

Abstract—The pink clays from the Tagus basin, Spain, were characterized by X-ray difraction (XRD), infrared spectroscopy (IR), scanning electron microscopy (SEM), and transmission electron microscopy (TEM). Chemical data were obtained by plasma emission spectroscopy and analytical electron microscopy (AEM), and specific surface and cation-exchange capacity were measured also. The data indicate that these pink clays are primarily stevensite. This Mg-rich smectite is characterized by poor crystallinity, a high degree of structural disorder, trioctahedral character (pure magnesian), a very low cation-exchange capacity, a very small crystal size (which generates an abnormally high specific surface area), and a deficiency of octahedral cations. On the basis of the very small crystal size, a large number of edge dislocations, the lack of periodicity (turbostratic) in the structure, and a cellular (spherical) texture observed by TEM, we consider this occurrence to be an early stage of crystallization. Unlike other precursor clay materials described in the literature, this clay is not an alteration of volcanic ash, but it was generated by precipitation from a Si- and Mg-saturated medium.

Key Words—Precursor Clay, Smectite, Stevensite, Tagus Basin (Spain), Incipient Crystallization.

INTRODUCTION

The Tagus basin is an intramontane basin located in the central Iberian Peninsula. The basin is partially filled by Tertiary sediments deposited within a complex system of alluvial fans. These sediments, distributed in a concentric pattern, are weathering products of igneous, metamorphic, and calcareous rocks from peripheral mountains. Detrital facies occur near the margins of the basin, and the core of the basin is mainly saline, with intermediate zones consisting of mud-flat facies. The nature, distribution, and characteristics of the different facies were described by Bellanca *et al.* (1992), Calvo Sorando *et al.* (1989), Domínguez Díaz (1994), and others.

The objective of this work is to study the "pink clays", which occur as interlayered strata in the "Green Clays Unit" as defined by Brell *et al.* (1985). They form part of the mud-flat facies (transition zone of the alluvial-fans system). Previous mineralogical studies (Brell *et al.*, 1985; Doval *et al.*, 1985; García Romero *et al.*, 1990; Domínguez Díaz, 1994) showed that the pink clays are mostly magnesian 2:1 phyllosilicates, similar to saponites belonging to the "Green Clays Unit". However, details of the mineralogy, microstructure, and physico-chemical properties are different from saponite. The mineralogy of the pink clays remains unclear although they have been studied by X-ray diffraction (XRD), infrared spectroscopy (IR), and optical microscopy Brell *et al.* (1985) described them as chlorite-smectite interstratified minerals. Conversely, García Romero (1988) and García Romero *et al.* (1988, 1990) called them pure stevensite. Martín de Vidales *et al.* (1988) showed that they are composed of pure magnesian 2:1 phyllosilicates of "intermediate character" between end-member kerolite and a Mg-rich smectite phase. On the other hand, Martín de Vidales *et al.* (1991) and Cuevas (1991) suggested that the same clays were composed of kerolite-stevensite interstratifications with variable stevensite content. Pozo *et al.* (1992, 1996) and Pozo and Casas (1995) agreed that the clays contained kerolite-stevensite interstratified minerals. This paper provides the first transmission electron microscopic (TEM) observations of these materials to better define the minerals present.

MATERIAL AND METHODS

Sampling was performed in three profiles: at Magán, Esquivias, and Valdemoro villages (Figure 1) where pink clays are interlayered between green saponitic clay layers. In general, the "Green Clays Unit" is 8–10 m thick and is composed of massive or bioturbated green or greenish-grey clays with intercalations of fining-upwards micaceous sands showing a thin parallel lamination. These green clays, which are mined commercially as bentonites, are mainly composed of phyllosilicates with minor feldspar and quartz. Most of these phyllosilicates (75–90%) are saponites with <10% illite (García Romero *et al.* 1988, 1990; Santiago Buey *et al.*, 1998).

The interlayered pink-clay strata decrease in total thickness from 1.5–2 m in the Esquivias and Valdemoro zones to a few centimeters in the south of the basin (Magán). They usually appear as massive beds, with interlayered carbonates of little lateral continuity

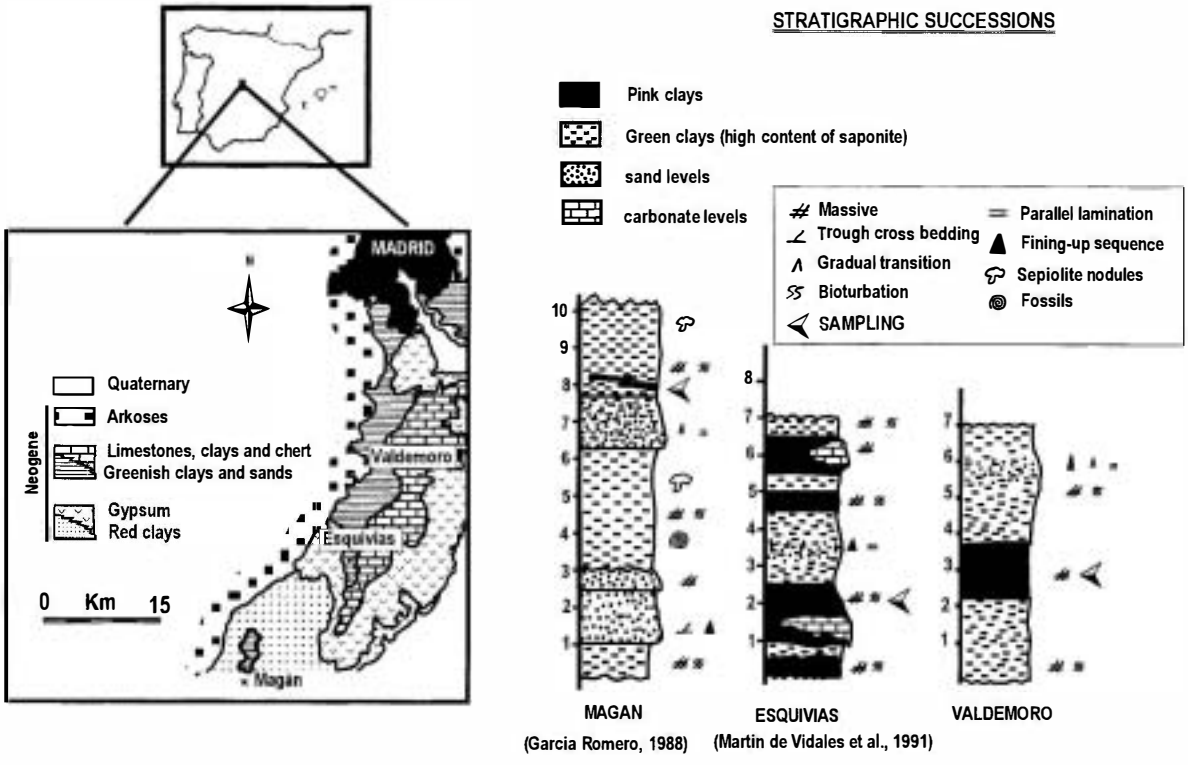

Figure 1. Map showing the geographic and geological setting of the studied material.

and become more abundant near the top (García Romero *et al.*, 1988, 1990).

Methodology

Mineralogical identification was performed by XRD in a Philips 1130/90 diffractometer using CuKα radiation and a graphite monochromator. Random powders were scanned from 2 to 65 °2θ at a 0.16 °2θ/s scan speed and oriented aggregates (<2-μm size fraction) were scanned from 2 to 18 °2θ at a 0.33 °2θ/s scan speed.

IR absorption spectra were obtained on a BIO RAD SPC 3200 instrument, using the KBr pellet technique from 4000 to 500 cm^{-1}. Elemental analyses were performed by plasma emission spectroscopy, using a Perkin-Elmer emission spectrometer, model Plasma II. Previous to the analysis, solids were digested under pressure in a nitric-hydrofluoric acid mixture, contained in a polytetrafluoroethylene (PTFE) autoclave. Additional elemental X-ray microanalyses from isolated particles were obtained by analytical electron microscopy (AEM).

Information about the oxidation states of the iron was obtained by Mössbauer spectroscopy. Room-temperature (291 ± 1 K) absorption spectra were obtained with Mössbauer "Perseus" spectrometer of Russian origin. In this spectrometer, the stabilization and the control of vibrator velocity are obtained via laser interferometer. A source of ^{57}Co in a Cr matrix was used. The spectra were measured in the velocity interval ± mm/s^{-1}.

Particle morphology and texture were observed by scanning electron microscopy (SEM). SEM observations were performed with a JEOL JSM6400 operated at 20 kV and equipped with a Link eXL X-ray energy dispersive detector. Samples were air-dried and then oven-dried at 40–60°C until constant weight. Finally, and prior to observation, they were lightly coated with gold.

TEM studies were performed with undisturbed specimens that presumably retain original textures. Oriented sections were prepared according to the method of Tessier (1984) which minimizes dehydration during TEM observation. The resulting epoxy-clay complexes are sectioned by ultramicrotomy (50 nm thick). The TEM observations were performed in a JEM 2000FX microscope operated at 200 kV and equipped with a Link AN10000 X-ray energy dispersive detector.

The exchange cations were extracted with NH_4^+ and the cation-exchange capacity (CEC) was calculated using distillation and measurement of NH_4^+ by the Kjeldaljh method, without removing soluble salts (Santos, 1979). The specific surface area was determined from a Micrometritics ASAP 2010 analyzer, after outgassing the sample at 110°C for 8 h to a residual pressure

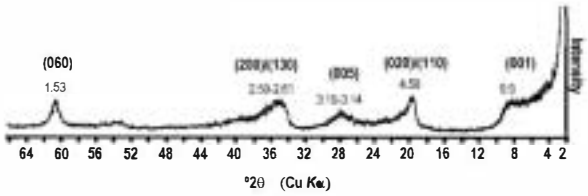

Figure 2. Representative XRD powder pattern of the pink clays.

of 10^{-5} mm Hg. The Brunauer-Emmett-Teller (BET) method was used for the calculation (Brunauer *et al.*, 1938).

RESULTS AND DISCUSSION

Figure 2 shows a representative XRD pattern where a very broad diffraction effect at low angles can be seen. This effect was also described by Martín de Vidales *et al.* (1991). These authors assumed this phenomenon is related to particle-size and textural features (*i.e.*, stacking disorder). This XRD powder pattern is composed of (*hk*0) and (00*l*) broad and asymmetrical bands instead of discrete reflections, which may be related to the lack of three-dimensional periodicity because of random rotations or translations between layers, giving rise to extensive stacking disorder. Also, partial hydration of the sample can produce broadening of the basal reflections. The *b*-axis dimension estimated from the (060) reflection is 9.18 Å, which indicates the material is trioctahedral. No nonclay minerals were detected.

Figure 3 shows a representative X-ray diffraction pattern of the oriented clay aggregate of <2 μm (air-dried, glycolated, and heated). Low-angle scattering (≤8.8 °2θ) is observed in all the cases. This band may be produced by different interlayer materials in the sample. Samples solvated with ethylene glycol swell slightly. Also, when heated at 550°C, the spacings collapse slightly. These phenomena are observed by the displacement of the band towards lower or higher angles, respectively. The 002 and higher peaks are missing in the pattern indicating the lack of periodic stacking of layers along the [001] direction. The absence of a well defined 001 reflection makes it impossible to calculate a crystallinity index or mean crystal size. Although the smectitic nature of the clays and the trioctahedral character of the mineral can be determined by XRD, the broad reflections (Martín de Vidales *et al.*, 1991) suggest that these materials have limited coherent domains with a very small number of layers per particle (*i.e.*, poor crystallinity or high structural disorder).

The IR data show intense and complex OH-stretching bands (4000–3000 cm^{-1}) owing to hydroxyl groups and H_2O molecules (Figure 4). These bands indicate a large amount of H_2O associated in different ways with the structure, as is typical for minerals of

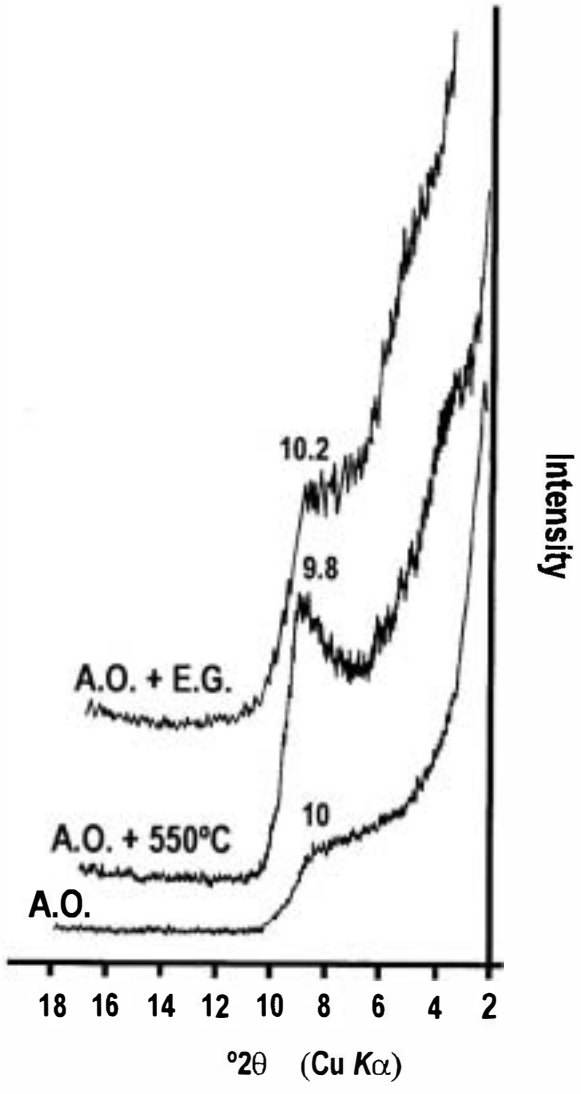

Figure 3. Representative XRD pattern of the oriented aggregate of clay fraction <2 μm. Air-dried (O.A.), glycolated (O.A. + EG), and heated (O.A. + 550°C).

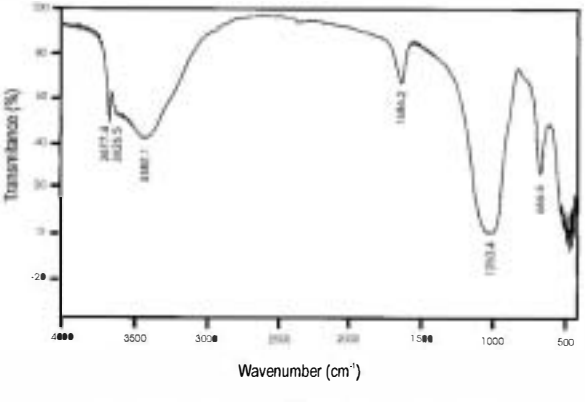

Figure 4. IR spectrum of the pink clays.

Table 1. Whole-rock chemical analyses of saponite, sepiolite, two stevensites, a saponite from the Tagus basin, and from pink clay material studied here.

Oxide	Saponite[1]	Saponite[2]	Sepiolite[3]	Stevensite[4]	Stevensite[5]	This study[6]
SiO_2	48.96	55.60	54.56	57.30	57.24	55.03 ± 2
TiO_2	0.20	0.62	—	—	—	0.07 ± 0.0005
Al_2O_3	7.30	13.52	0.99	—	—	2.13 ± 0.01
Fe_2O_3	11.93	3.63	1.56	0.32	1.14	0.94 ± 0.003
FeO	1.24	0.91	0.88	—	0.12	0.24 ± 0.003
MnO	—	0.04	3.02	0.21	0.75	0.01 ± 0.0001
MgO	23.39	21.58	21.72	27.47	27.89	24.01 ± 0.2
CaO	2.42	0.93	0.00	0.97	0.38	0.01 ± 0.004
Na_2O	0.04	0.78	0.01	0.03	—	0.03 ± 0.003
K_2O	0.06	2.30	0.02	0.03	—	0.04 ± 0.01
H_2O (+)	—	12	9.23	6.69	7.69	16.32
H_2O (−)	4.45	—	7.92	7.17	4.76	—

[1] Winnweiler, Pflaz, Germany (Quakernaat, 1970).
[2] Tagus basin, Spain (Santiago Buey *et al.,* 1998).
[3] Akatani Mine (Otsuka *et al.,* 1966).
[4] Springfield (Faust and Murata, 1953).
[5] Jersey City (Faust and Murata, 1953).
[6] Tagus basin, Spain (This paper, pink clays).

the smectite group. The spectrum in the OH region of the unheated material shows a sharp absorption band at 3677 cm^{-1} and a broad band at 3382 cm^{-1} with a shoulder at 3626 cm^{-1}. The absorption band at 3677 cm^{-1} is assigned to the OH-stretching vibration in purely magnesian octahedral sheets (OH-Mg-Mg) (Farmer, 1974; Van der Marel, 1976). The broad bands at 3626 and 3382 cm^{-1} are attributed to the OH-stretching vibration of interlayer and hygroscopic H_2O, respectively. Absorption corresponding to the bending vibration of H_2O molecules (atmospheric moisture) occurs at 1636 cm^{-1} as a single band. In the lower frequency region from 700 to 1200 cm^{-1}, the Si-O stretching absorption appears at ~1050 cm^{-1} as a strong and broad band, which is common to silicates (Faust *et al.,* 1959). In addition to this band, the Si-O-Mg bending band at 666 cm^{-1} was observed. From the smectite group, stevensite is the only mineral which exhibits this absorption band, but it is typical of talc and sepiolite as well (Faust *et al.,* 1959).

The OH-Mg-Mg stretching band at 3677 cm^{-1} and the Si-O-Mg bending band at 666 cm^{-1} are related to Mg in the octahedral sheet and correspond to a pure magnesian smectite, sepiolite, or talc (Farmer, 1974; Van der Marel, 1976). The total absence of Al-related bands at 919–915 cm^{-1} (Al-Al-OH) and 527–517 cm^{-1} (Si-O-Al) (Madejova *et al.,* 1992; Vicente-Rodríguez *et al.,* 1996) suggests the absence or near absence of saponite.

Chemical analyses obtained by plasma spectroscopy are summarized in Table 1. For comparison, selected analyses from the literature are presented also. The pink clays studied in this work have a lower Mg content than talc and kerolite and higher Al content than other stevensites.

Because the XRD data indicate that this material is a nearly pure 2:1 phyllosilicate, the structural formula was calculated based on $O_{20}(OH)_4$ as: $Si_{8.01}O_{20}(Al^{3+}_{0.36}Fe^{3+}_{0.11}Fe^{2+}_{0.03}Mg^{2+}_{4.76})(OH)_4(Mg_{0.45}Na_{0.01}K_{0.01})$. This formula corresponds to stevensite with an extremely low CEC (generated by a deficiency of octahedral cations in the structure, and not by isomorphous substitutions) or an interstratified clay. The latter possibility agrees with Martín de Vidales *et al.* (1991), Cuevas (1991), Pozo *et al.* (1992, 1996), and Pozo and Casas (1995).

Because the whole-rock chemical analysis corresponds to the entire sample and it is not possible to exclude contamination by impurities not detected by XRD, AEM analyses were performed on 68 isolated particles to determine the distribution of elements between grains. Some heterogeneity of Si, Mg, Al, and Fe is observed between individual particles, indicating a mixture of different minerals. Most of the analyses (~85%) correspond to stevensite with a negligible amount of aluminum in the tetrahedral sheet and a deficiency of atoms (<6) in octahedral coordination (Faust *et al.,* 1959). In addition, talc (~10%) and saponite (~5%) particles were found. Chemical analyses in wt. % for the purest particles of each of the three minerals are listed in Table 2.

The presence of muscovite (<1%) and saponite (~5%) generates most of the Al detected by plasma spectroscopy in the whole rock. Some particles were found with an anomalously high quantity of SiO_2 or MgO as detected by AEM. This may be caused by SiO_2 or Mg adsorbed on the surface of the particles (Jones, 1985) or by SiO_2 and MgO as a coating.

Isolated particle analyses are represented in Figure 5. For comparison, the theoretical fields of trioctahed-

Table 2. Chemical analyses in wt. % for the purest particles of stevensite, talc, and saponite found in the pink clays.

Oxide	Stevensite	Talc	Saponite
SiO_2	64.73	63.05	53.77
TiO_2	—	—	—
Al_2O_3	3.15	—	15.46
Fe_2O_3	2.11	—	6.51
FeO	0.52	—	1.63
MnO	—	36.94	—
MgO	24.68	—	15.48
CaO	1.58	—	2.63
Na_2O	1.84	—	1.76
K_2O	1.38	—	2.76

ral phyllosilicate minerals are given also. The grains cluster in or near the theoretical compositions of talc, stevensite, and saponite, respectively. Although some particles have sepiolite composition, no fibrous particles were observed.

The CEC of the pink clays in 23 meq/100 g. This exchange capacity is very low with respect to most smectites, but is in accordance with other determinations for stevensite. For example, Faust *et al.* (1959) reported an exchange capacity of 37.6 meq/100 g and Tettenhorst and Moore (1978) reported 30 meq/100 g for the stevensites they studied. Partly in recognition of a low CEC, Faust and Murata (1953) defined stevensite as a mineral of the montmorillonite group, with a low CEC arising from a deficiency in octahedral cations rather than from other isomorphous substitutions. The main exchangeable cations are Mg (10.4 meq/100 g), Ca (9.8 meq/100 g), Na (1 meq/100 g), and K (0.4 meq/100g).

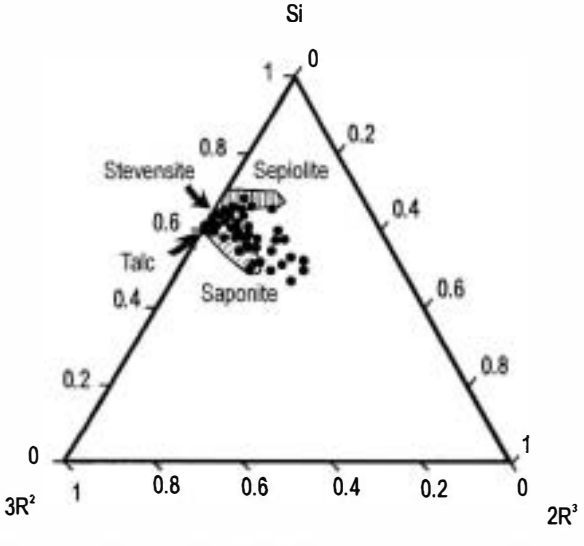

Figure 5. Ternary Si-$3R^2$-$2R^3$ diagram of analyses obtained by analytical electron microscopy and showing the theoretical field for trioctahedral minerals $3R^2 = [(Mg^{2+} + Fe^{2+})/3]$, $2R^3 = [(Al^{3+} + Fe^{3+}) - (Na^+ + K^+ + 2Ca^{2+})]/2$ (after Velde, 1985).

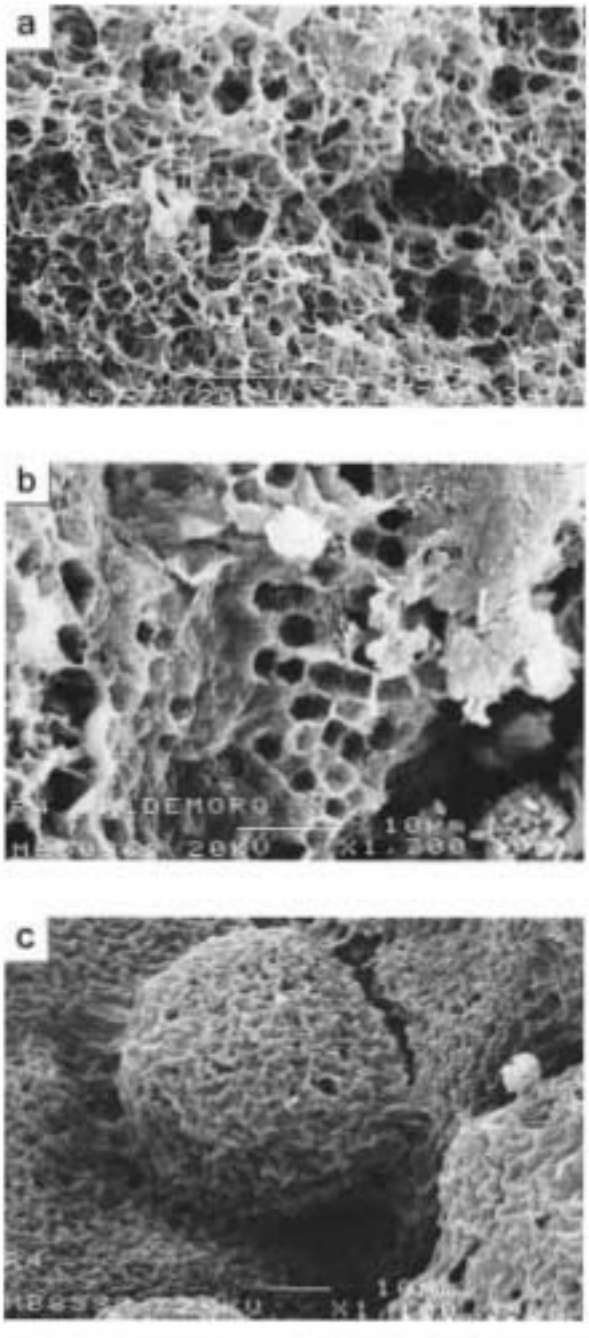

Figure 6. a) Random array of smectite particles (honeycomb microstructure). b) Edge-to-edge and edge-to-face contacts between particles. c) Spherical aggregates of particles.

The specific-surface area obtained (N_2-BET) is high (392 m^2/g) owing to external surfaces of the particles (314 m^2), and the remaining area (78 m^2) corresponds to internal (interlayer) surfaces. Thus, an extremely small crystallite size is deduced, in agreement with incipient crystal growth.

In general, a nearly isotropic fabric is observed, formed by a random (non-oriented) array of very small

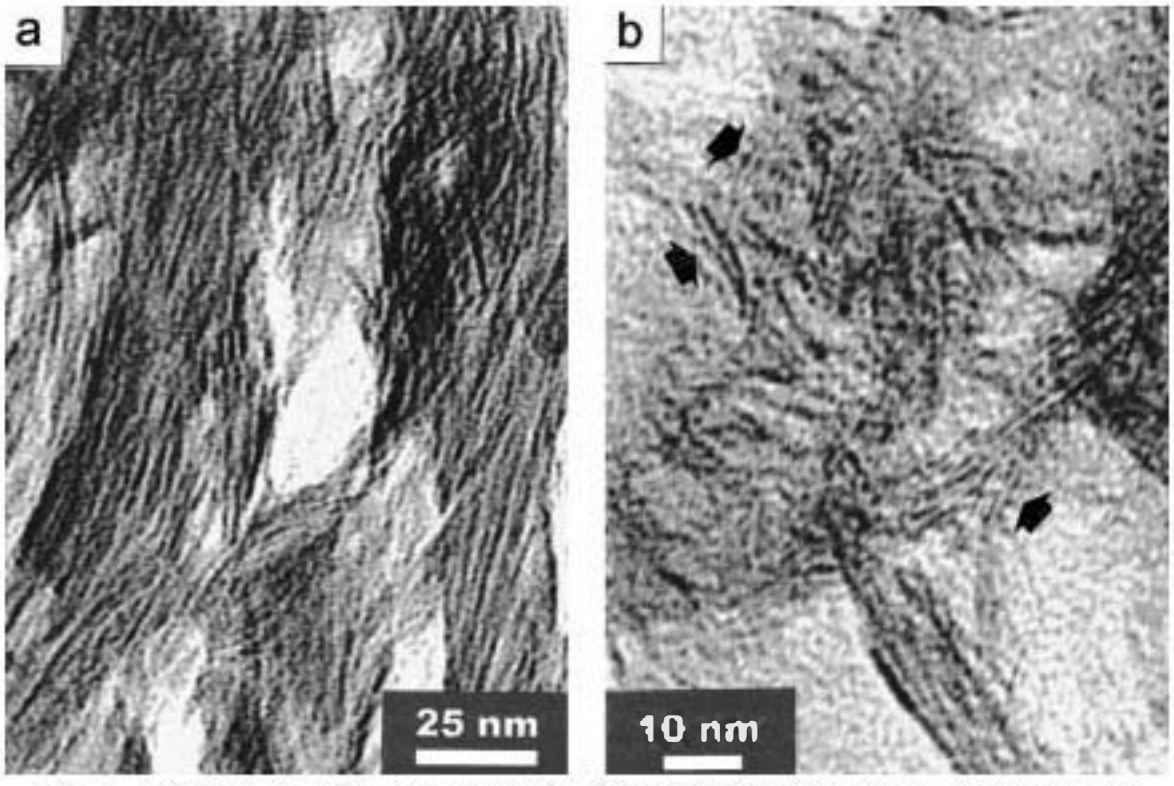

Figure 7. a) Anastomosing and wavy fringes with edge dislocations. b) Colloidal plasma comprised of monolayers.

smectite particles (Figure 6a). This microstructure is typical of high-swelling soils with high salt concentrations that reduce interparticle repulsion (Bennett and Hulbert, 1986; van Olphen, 1966). Most samples have open structures with pseudo-polygonal voids ("cornflake" and "honeycomb" microstructure) formed of smectite laminar particles, which keep edge-to-face and edge-to-edge contacts (the latter are more abundant) (Figure 6b). This texture explains the very low density of the rock (0.7–0.8 g/cm³). Elsewhere, smectite particles show a tendency to be connected by forming flocs or aggregate structures with spherical morphologies (cellular texture) separated by voids of varying sizes and shapes (Figure 6c).

TEM micrographs show broad, poorly defined fringes varying from 10 to 12 Å thick. The particles have wavy, anastomosing, and discontinuous lattice-fringe images (Figure 7a and 7b) with a high number of edge dislocations and changes in image contrast along the layers, owing to small orientation changes in the crystal (Banfield and Eggleton, 1988). The heterogeneity and wavy structure of the lattice fringes are consistent with sample formation in relatively shallow water environments where crystallization occurred relatively rapidly at low temperatures.

In addition, TEM micrographs show a common structure of hollow-packed spheres (Figure 8), having apparent diameters ranging from 50 to 1000 Å. Some sphere walls display a concentric layered structure. This cellular texture resembles descriptions of primitive clay precursors forming from glasses, gels, or weathering of previous minerals. For example, Eggleton and Bunsick (1980) studied precursors of smectite in the alteration of K-rich feldspar. They found a cellular texture of packed hollow spheres with matter layered concentrically around the bubbles. They postulated that the bubble diameter exerted a control on the rate of crystallization of the bubble walls. Later, Eggleton (1987) studied the formation of these structures in the crystallization process of clay minerals from noncrystalline Fe-Si-Al-rich oxyhydroxides. He proposed that the layer structure within the walls of the bubbles indicates incipient development of crystals. Tazaki and Fyfe (1987) and Tazaki *et al.* (1989) observed well-ordered domains with spherical structures. They concluded also that the structures were early stages of crystallization within volcanic glass, and must be precursors from which clay develops. Masuda *et al.* (1996) studied a precursor as an intermediate stage in the formation of authigenic smectite from volcanic glass. Kawano *et al.* (1997) examined the formation processes of clay minerals by transformation from noncrystalline Al-hydroxide gels, which precipitated from solutions in early weathering of volcanic glass, leading to crystalline materials.

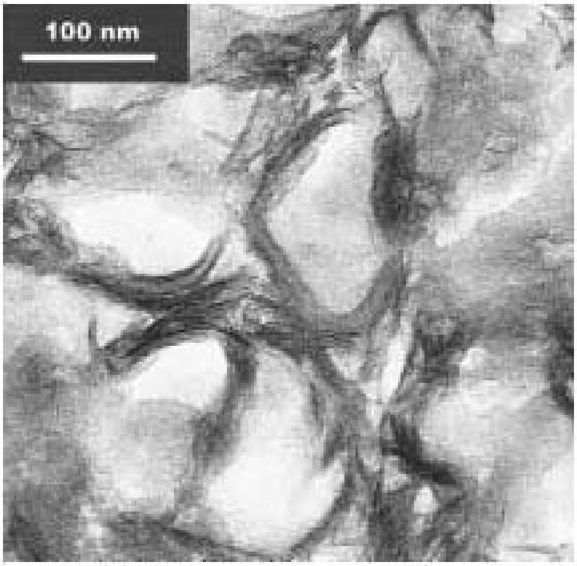

Figure 8. TEM micrograph showing a structure dominated by packed hollow spheres (cellular texture).

These previous studies, in agreement with our observations of the pink clays, describe poorly crystalline particles with textures of hollow-packed spheres. The wall material of these spheres contains poorly crystallized matter which may develop clay minerals. These particles are referred to here as "precursor-clay material" and are inferred to be incipient nucleation sites of very fine-grained, smectite-like regions. These regions have cellular texture, a high density of edge dislocations, and very small crystallite sizes.

The cellular texture described in this work is not inherited from volcanic ash. The distinguishing feature of this pink clay is related to its sedimentary origin. There is no possibility of volcanic influence in its formation and, therefore, there is no previous texture which can be inherited. The sedimentary origin of this clay by precipitation in an intracontinental basin is well known (Bellanca *et al.*, 1992; Brell *et al.*, 1985; Calvo Sorando *et al.*, 1989; Domínguez Díaz, 1994; García Romero, 1988; García Romero *et al.*, 1990) and, as far as we are aware, this is the first time this cellular texture is observed terials.

CONCLUSIONS

The characterization of the pink clays from the Tagus basin, Spain, was accomplished by several techniques of which the TEM observations were the most important. TEM data indicate that the presence of a kerolite-stevensite interstratification phase does not occur as previous authors have argued by using XRD, IR, and optical microscopy data (Martín de Vidales *et al.*, 1988, 1991; Cuevas, 1991; Pozo *et al.*, 1992, 1996; Pozo and Casas, 1995). In contrast, our view is that this material is composed of almost pure Mg-rich stevensite. Some heterogeneity in the distribution of the major elements between particles, and the consequent charge variation, produces a mixture of predominant stevensite particles with small amounts of saponite and talc particles.

Pink clays are mainly composed of stevensite showing the following properties: a variable >10-Å interlayer spacing, and the layer charge arises from a deficiency in octahedral cations rather than from cation substitutions (in agreement with Faust and Murata, 1953; and Faust *et al.*, 1959). Furthermore, there is inhomogeneity in the sequence of layers which makes a detailed interpretation of the structure difficult to obtain (Brindley, 1955). However, TEM observation rules out the possibility of smectite-talc interstratification. There is no well-developed layer stacking and there is no alternation of spacings along the stacking direction. Thus, this material cannot be an interstratified mineral.

The boundary between kerolite, approximately: $Si_4O_{10}(Mg,Al,Fe)_3(OH)_2(H_2O)$ and the pink clay reported here: $Si_{3.91}O_{10}(Al^{3+}_{0.10}Fe^{3+}_{0.11}Fe^{2+}_{0.02}Mg^{2+}_{2.70})(OH)_2(Mg_{0.0?}Na_{0.01}K_{0.01})$ may be indistinguishable, both because the chemistries are close and an accurate chemical determination is difficult. XRD and IR data are not diagnostic. We confirm the smectitic nature of the pink clays by means of its swelling potential as observed by

ACKNOWLEDGMENTS

The authors thank R.E. Ferrell, Jr. for comments which did much to improve both the form and the content of this paper. The electron microscopy study was performed at the Centro de Microscopía Electrónica "Luis Bru" (U.C.M.). We acknowledge the technical assistance of E. Baldonedo and J. González.

REFERENCES

Banfield, J.F. and Eggleton, R.A. (1988) Transmission electron microscope study of biotite weathering. *Clays and Clay Minerals*, **36**, 47–60.

Bellanca, A., Calvo, J.P., Censi, P., Neri, R., and Pozo, M. (1992) Recognition of lake-level changes in miocene lacustrine units, Madrid basin, Spain. Evidence from facies analysis, isotope geochemistry and clay mineralogy. *Sedimentary Geology*, **76**, 135–153.

Barnett, R.H. and Hulbert, M.H. (1986) *Clay Microstructure*. D. Reidel Publishing, Boston, 161 pp.

Brell, J.M., Doval, M., and Caramés, M. (1985) Clay mineral distribution in the evaporitic Miocene sediments of the Tajo basin, Spain. *Mineralogica et Petrographica Acta*, **29**, 267–276.

Brindley, G.W. (1955) Stevensite, a montmorillonite mineral showing mixed-layer characteristics. *American Mineralogist*, **40**, 239–247.

Brunauer, S., Emmet, P.H., and Teller, E. (1938) Adsorption of gases in multimolecular layers. *Journal of the American Chemical Society*, **60**, 309–319.

Calvo Sorando, J.P., Alonso Zarza, A.M., and García del Cura, M.A. (1989) Models of miocene marginal lacustrine

sedimentation in response to varied depositional regimes and source areas in the Madrid basin (central Spain). *Paleogeography, Paleoclimatology, Palaeoclimatology, Palaeoecology,* **70,** 199–214.

Cuevas, J. (1991) *Caracterización de las Esmectitas Magnésicas de la Cuenca de Madrid como Material de Sellado. Alteración Hidrotermal.* ENRESA technical publication nº 04/92.

Domínguez Díaz, M.C. (1994) Mineralogía y sedimentología del neógeno del sector centro occidental de la cuenca del Tajo. Ph.D. thesis, Universidad Complutense de Madrid, Spain, 397 pp.

Doval, M., Domínguez Díaz, M.C., Brell, J.M., and García Romero, E. (1985) Mineralogía y sedimentología de las facies distales del borde norte de la cuenca del Tajo. *Boletín de la Sociedad Española de Mineralogía,* **8,** 257–269.

Eggleton, R.A. (1987) Non-crystalline Fe-Si-Al-oxyhydroxides. *Clays and Clay Minerals,* **35,** 29–37.

Eggleton, R.A. and Buseck, D.R. (1980) High-resolution electron microscopy of feldspar weathering. *Clays and Clay Minerals,* **28,** 173–178.

Farmer, V.C. (1974) *The Infrared Spectra of Minerals.* Mineralogical Society of Great Britain, London, 539 pp.

Faust, G.T. and Murata, K.J. (1953) Stevensite, redefined as a member of the montmorillonite group. *American Mineralogist,* **38,** 973–987.

Faust, G.T., Hathaway, J.C., and Millot, G. (1959) A restudy of stevensite and allied minerals. *American Mineralogist,* **44,** 342–370.

Garcia Romero, E. (1988) Estudio mineralogico y estratigráfico de las arcillas de las facies centrales del neógeno del borde sur de la cuenca del Tajo. Ph.D. thesis, Universidad Complutense de Madrid, Spain, 356 pp.

García Romero, E., Brell, J., Doval, M., and Perruchot, A. (1988) Características y evolución de la sedimentación neógena en la región de la Sagra (cuenca del Tajo). *Boletín de la Real Sociedad Española de Historia Natural (Geología),* **84,** 85–99.

García Romero, E., Brell, J.M., Doval, M., and Navarro, J.V. (1990) Caracterización mineralógica y estratigráfica de las formaciones neógenas del borde sur de la cuenca del Tajo (comarca de la Sagra). *Boletín Geológico y Minero,* **101,** 945–956.

Jones, B.F. (1985) *Clay Mineral Diagenesis in Lacustrine Sediments.* U.S. Geological Survey Bulletin 1578, Washington, D.C., 291–300.

Kawano, M., Tomita, K., and Shinohara, Y. (1997) Analytical electron microscopic study of the noncrystalline products formed at early weathering stages of volcanic glass. *Clays and Clay Minerals,* **45,** 440–447.

Madejová, J., Putyera, K., and Cicél, B. (1992) Proportion of central atoms in octahedra of smectites calculated from infrared spectra. *Geologica Carpathica, Clays,* **2,** 117–120.

Martín de Vidales, J.L., Pozo, M., Medina, J.A., and Leguey, S. (1988) Formación de sepiolita-paligorskita en litofacies lutítico-carbonáticas en el sector de Borox-Esquivias (Cuenca de Madrid). *Estudios Geológicos,* **44,** 7–18.

Martín de Vidales, J.L., Pozo, M., Alía, J.M., García Navarro, F., and Rull, F. (1991) Kerolite-stevensite mixed-layers from the Madrid basin, central Spain. *Clay Minerals,* **26,** 329–342.

Masuda, H., O'Neil, J.R., Jiang, W., and Peacor, D.R. (1996) Relation between interlayer composition of authigenic smectite, mineral assemblages, I/S reaction rate and fluid composition in silicic ash of the Nankai trough. *Clays and Clay Minerals,* **44,** 443–459.

Otsuka, R., Imai, N., and Nishikawa, M. (1966) On the dehydration of sepiolite from the Akatani mine. Niigata prefecture, Japan. *Journal of the Chemical Society of Japan (Industrial Chemistry Society),* **66,** 1677–1680.

Pozo, M. and Casas, J. (1995) Distribución y caracterización de litofacies en el yacimiento de arcillas magnésicas de esquivias (neógeno de la cuenca de Madrid). *Boletín Geológico y Minero,* **106,** 265–282.

Pozo, M., Casas, J., Moreno, A., and Medina, J.A. (1992) Origin of sedimentary magnesium bentonites in marginal lacustrine deposits (Madrid basin, Spain). *Chemical Geology,* **107,** 457–461.

Pozo, M., Moreno, A., Casas, J., and Martín Rubí, J.A. (1996) Estudio geoquímico de litofacies con arcillas magnésicas en depósitos lacustres-palustres de la cuenca de Madrid. *Boletín de la Sociedad Española de Mineralogía,* **19,** 71–83.

Quakernaat, J. (1970) A new occurrence of a macrocrystalline form of saponite. *Clay Minerals,* **8,** 491–493.

Romero, R., Robert, M., Elsass, F., and García, C. (1992) Evidence by transmission microscopy of weathering microsystems in soils developed from crystalline rocks. *Clay Minerals,* **27,** 21–33.

Santiago Buey, C., Suárez Barrios, M., García Romero, E., Doval Montoya, M., and Domínguez Díaz, M.C. (1998) Electron microscopic study of the bentonites from "Cerro del Aguila" (Toledo, Spain). *Clay Minerals,* **33,** 501–510.

Santos, F. (1979) Estudio geológico y edafológico del sector Montiel-Alcaraz-Bienservida (Ciudad Real—Albacete). II. Estudio edafológico. Ph.d. thesis, Universidad de Granada, Spain, 489 pp.

Shimoda, S. (1971) Mineralogical studies of a species of stevensite from the Obori mine, Yamagata prefecture, Japan. *Clay Minerals,* **9,** 185–192.

Tazaki, K. and Fyfe, W.S. (1987) Primitive clay precursors formed on feldspar. *Canadian Journal of Earth Science,* **24,** 506–527.

Tazaki, K., Fyfe, W.S., and van der Gaast, S.J. (1989) Growth of clay minerals in natural and synthetic glasses. *Clays and Clay Minerals,* **37,** 348–354.

Tessier, D. (1984) Etude de l'organisation des matériaux argileux. Hydration, gonflement et structuration au cours de la dessiccation et de la rehumectation. Ph.D. Thesis, Universite de Paris VII, Paris, 361 pp.

Tettenhorst, R. and Moore, G.E., Jr. (1978) Stevensite oolites from the Green River Formation of central Utah. *Journal of Sedimentary Petrology,* **48,** 587–594.

van der Marel, H.W. (1976) *Atlas of Infrared Spectroscopy of Clay Minerals and Their Admixtures.* Elsevier, Amsterdam, 396 pp.

van Olphen, H. (1966) *An Introduction to Clay Colloid Chemistry: For Clay Technologists, Geologists and Soil Scientists.* Interscience Publishers, New York, 301 pp.

Velde, B. (1985) *Clay Minerals. A Physico-Chemical Explanation of Their Occurrence.* Elsevier, Amsterdam, 427 pp.

Vicente-Rodriguez, M.A., Suárez, M., Bañares-Muñoz, M.A., and López-González, J. de D. (1996) Comparative FT-IR study of the removal of octahedral cations and structural modifications during acid treatment of several silicates. *Spectrochimica Acta, Part A,* **52,** 1685–1694.

E-mail of corresponding author: cristina@eucmax.sim.ucm.es